Current Research in Food Science 7 (2023) 100620

Contents lists available at ScienceDirect

Current Research in Food Science

journal homepage: www.sciencedirect.com/journal/current-research-in-food-science

Enhanced electric field and charge polarity modulate the microencapsulation and stability of electrosprayed probiotic cells (*Streptococcus thermophilus,* ST44)

Panagiota Dima, Peter Reimer Stubbe, Ana C. Mendes *, Ioannis S. Chronakis **

Technical University of Denmark, DTU-Food, Research Group for Food Production Engineering, Lab. of Nano-BioScience, B202, 2800, Kgs Lyngby, Denmark

ARTICLE INFO

Keywords:
Lactic acid bacteria
Streptococcus thermophilus
Maltodextrin
Encapsulation
Electrohydrodynamics
Numerical simulation

ABSTRACT

The effect of the polarity of the direct current electric field on the "organization" of *Streptococcus thermophilus* (ST44) probiotic cells within electrosprayed maltodextrin microcapsules was investigated. The generated electrostatic forces between the negatively surface-charged probiotic cells and the applied negative polarity on the electrospray nozzle, allowed to control the location of the cells towards the core of the electrosprayed microcapsules. This "organization" of the cells increased the evaporation of the solvent (water) and successively the glass transition temperature (Tg) of the electrosprayed microcapsules. Moreover, the utilization of auxiliary ring-shaped electrodes between the nozzle and the collector, enhanced the electric field strength and contributed further to the increase of the Tg. Numerical simulation, through Finite Element Method (FEM), shed light to the effects of the additional ring-electrode on the electric field strength, potential distribution, and controlled deposition of the capsules on the collector. Furthermore, when the cells were located at the core of the microcapsules their viability was significantly improved for up to 2 weeks of storage at 25 °C and 35% RH, compared to the case where the probiotics were distributed towards the surface. Overall, this study reports a method to manipulate the encapsulation of the surface charged probiotic cells within electrosprayed microcapsules, utilizing the polarity of the electric field and additional ring-electrodes.

1. Introduction

Probiotics are living microorganisms that have been proven to exert health benefits on the host when consumed in adequate numbers (Terpou et al., 2019). Commonly known probiotics that have therapeutic effects on humans are the Lactic Acid Bacteria (LAB) (Parvez et al., 2006). One example of LAB with probiotic potential is *Streptococcus thermophilus*, which has been associated with health benefits including anti-inflammatory effects, antimutagenic effects, and stimulation of the gut immune system among others (Martinović et al., 2020; Zhang et al., 2020). ST44 is an industrially relevant strain, since it is commonly used as a dairy starter bacterium (Padmanabhan et al., 2020), thus it has been investigated and encapsulated in various studies (Ozturk et al., 2021; Pakroo et al., 2021; Vodnar et al., 2010).

In recent years the utilization of electrohydrodynamic atomization (electrospray and electrospinning) processing has been substantially explored for the encapsulation of probiotic cells (Mendes and Chronakis, 2021; Niamah et al., 2021). In our previous study, the encapsulation of the Gram-positive, rod-shaped *Bifidobacterium animalis* subsp. *lactis* (BB12) within maltodextrin microcapsules using both negatively and positively charged electrospray needle, was investigated (Dima et al., 2023). By choosing the appropriate polarity of DC electric field, the surface-charged probiotic cells were localized either in the core or towards the surface of the electrosprayed microcapsules, as observed using confocal microscopy. Negatively-charged probiotic cells, encapsulated using a negative polarity at the electrospray needle, were organized primarily in the core of the microcapsules. Moreover, the "organization" of the cells affected the evaporation of water and subsequently the glass transition temperature (Tg) of the electrosprayed capsules. The produced microcapsules using negative polarity showed considerably higher glass transition values (nearly 10 °C) and greater viability (~7.3 times higher) even after 3 days of storage at RH of 35% and 25 °C, compared to the encapsulated probiotics using positive polarity.

The conventional configuration of the capillary nozzle and grounded

* Corresponding author.
** Corresponding author.
E-mail addresses: anac@food.dtu.dk (A.C. Mendes), ioach@food.dtu.dk (I.S. Chronakis).

https://doi.org/10.1016/j.crfs.2023.100620
Received 5 June 2023; Received in revised form 20 September 2023; Accepted 18 October 2023
Available online 18 October 2023

substrate of the electrospray processing can be altered to prevent electric disturbances and improve the stability of electrospraying, as well as to focus the electrospray deposition (Kuwahata et al., 2020). The changes of the configuration could include the utilization of additional electrodes in the form of guard or extractor electrodes (coaxial with the capillary nozzle) of different shapes (rings, cylinders, plates of appropriate aperture) and sizes (Jaworek et al., 2018; Xie and Wang, 2007).

Additional ring electrodes in three-electrode arrangements (nozzle, ring electrode, collecting electrode) have been shown to modify the electric field and stabilize the electrospray process. Verdoold et al., reported that the changes of the electric field could be reflected on the properties of the current (i.e., relative standard deviation of the DC current, current mean–median ratio, pulse shape) through the electrospray system, the liquid meniscus, and subsequently the spraying mode (Verdoold et al., 2014). Zhao et al., reported that a three-electrode-arrangement caused changes of the electric field, providing a strong electric field with a fairly low voltage (Zhao et al., 2005). Moreover, Gan et al., suggested that the addition of a ring electrode, between a classical capillary-mesh electrode electrospray system, stabilized the process. Even though the electric field intensity around the capillary was weaker due to superposition principle of the electric field, the larger electric force produced from the ring electrode increased the droplet charge and reduced the droplet size and axial velocity (Gan et al., 2019). Moreover, it was reported that the driving force for the movement of droplets derived from the electric field between the ring electrode and the collector, while the produced capsules were more uniform, compared to the electrospraying system without the ring electrode, due to less axisymmetric disturbances (Gan et al., 2016).

The production of more uniformly sized capsules has also been described by Xie and Wang, who microencapsulated cells within sodium alginate gel beads by dripping mode electrospray. It was suggested that the additional ring electrode stabilized the performance of the electrospray system and facilitated the removal of undesired satellite droplets and the formation of larger droplets by decreasing the dripping frequency (Xie and Wang, 2007). In addition, Si et al., also reported that a coaxial needle assembly with two ring electrodes of different electric potential, gave rise to fine morphology (identifiable core–shell structure) and uniform size distribution of poly(D,L-lactide-co-glycolide) (PLGA) microparticles containing therapeutic agents. The additional two rings improved stability of the cone and expanded the process parameter (e.g., voltage, flow rate) range of the stable cone-jet mode (Si et al., 2013).

Numerical simulation tools are commonly employed to represent the electric field strength and electric potential distribution in an electrospray/electrospinning system. Neubert et al., investigated, both experimentally and numerically, the effect of additional ring-electrodes between the nozzle and the collector, on the controllable electrospun fiber deposition. They reported that the addition of a ring-electrode decreased the spot size that Nylon-6, poly(L-lactic acid)-co-poly-(3-caprolactone) (PLACL) and poly(vinyl chloride) (PVC) fibers were collected on the substate, due to the reduction of the lateral jet instabilities. The suppression of the bending instability onset resulted to a smaller electrospinning cone and, thus, a more focused collection on the substrate. The experimental conditions were also assessed by numerical modeling (SIMION) of the electric field distribution. It was confirmed that the utilization of two additional ring-electrodes focused further the collection of the fibers and decreased the modeled collection spot size (Neubert et al., 2012). Kuwahata et al., reported that the ternary ring electrode changed the electric potential around the nozzle and shifted the threshold voltage for single Taylor cone-jet formation, verifying their statement using a numerical simulation (Finite Element Method-FEM). Subsequently, the ring electrode facilitated the focusing of the spray plume and the controlling of the electrospray film deposition of Poly(lactic-co-glycolic acid) (PLGA) in N,N-dimethylformamide solution (DMF) (Kuwahata et al., 2020).

In our previous study, it was demonstrated that the encapsulation of the Gram-positive, rod-shaped, and hydrophobic *Bifidobacterium animalis* subsp. *lactis* within maltodextrin microcapsules, by electrospray, could be enhanced using negatively charged electrospray needle (Dima et al., 2023). However, the efficacy of this method has not been tested by using another distinct probiotic strain with different surface properties, size, and morphology from BB12. This study aimed at to investigate the effect of the electric field polarity and additional ring electrodes on the encapsulation and "organization" of coccus-shaped and hydrophilic *Streptococcus thermophilus* (ST44) probiotic cells within electrosprayed maltodextrin microcapsules. Maltodextrin, which is obtained by partial hydrolysis of starch, is a hydrophilic carrier and is commonly used as wall material for the encapsulation of probiotics (Mendes and Chronakis, 2021). Furthermore, to enhance the encapsulation process by electrospraying, the insertion of auxiliary ring-shaped electrodes was investigated. The "organization" of the probiotics as well as the glass transition of the electrosprayed microcapsules were tested under the different electrospray configurations. A numerical simulation using the Finite Element Method (FEM) was also employed, to evaluate the electric field strength and potential distribution between the electrospray needle and the collector, when auxiliary electrodes were utilized.

2. Materials and methods

2.1. Preparation of microorganisms

Probiotic cells *Streptococcus thermophilus* (ST44) of concentration 5.4 $\times$ 10^9 cells/g were supplied by Chr. Hansen A/S (Hørsholm, Denmark) and stored at −80 °C. The frozen probiotics' cell concentrate was thawed at room temperature (20 $\pm$ 1 °C) and was preliminary inoculated in 18 mL of M-17 broth (Merck KGaA, Darmstadt, Germany). After incubation for 24h at 37 °C under aerobic conditions (140 rpm), an additional amount of 20 mL fresh M-17 broth was inoculated with the bacterial preculture and incubated under the same conditions for 16h. Then the bacterial suspension was centrifuged at 3000g for 5min at 25 °C, and the cellular pellet was washed twice with demineralized water.

2.2. Atomic Force Microscopy (AFM) measurements

The AFM imaging (NanoWizard V, Bruker, Berlin, Germany) was performed in Quantitative Imaging mode using PEAKFORCE-HIRS-F-A scanning probe (Bruker, Camarillo, CA, USA). The ST44 probiotic cells were deposited on a surface of agarose coated glass, incubated, and gently rinsed with de-ionized water. The immobilized sample was then imaged in air.

2.3. Bacterial cell surface charge

The probiotic cells' surface electrical charge evaluation was performed according to a previously described protocol (Dertli et al., 2015; Dima et al., 2022). Approximately 10^8 ST44 probiotic cells/mL were suspended in 10 mM KH_2PO_4 (Sigma-Aldrich, Steinheim, Germany) and transferred to a capillary cell with gold plated beryllium/copper electrodes (DTS1070 cell, Malvern Panalytical Ltd, Malvern, UK). A Zeta-sizer (Malvern Panalytical Ltd, Malvern, UK) was utilized to measure the electrophoretic mobility of the samples, which was successively converted to zeta potential (mV) using the Helmholtz- Schmoluchowski equation.

$$U_p = V_p E = \zeta \varepsilon \eta \quad (1)$$

Where U_p is the electrophoretic mobility, V_p is the electrophoretic velocity, E is the electric field strength, ζ is the zeta potential, ε is the permittivity, and η is the viscosity of the medium.

All measurements were carried out at 25 °C and each sample was analyzed in quintuplicate.

2.4. Bacterial cell surface hydrophobicity

The surface hydrophobic/hydrophilic character of ST44 cells was assessed by the microbial adhesion to hexadecane (MATH) assay (Deepika et al., 2009). ST44 probiotic cells were suspended in 10 mM KH_2PO_4 until the optical density (turbidity) of bacterial suspensions at 600 nm (OD_{600})~0.8. An equal volume of 2 mL of the cell suspension and hexadecane (Thermo Fisher Scientific, Waltham, MA, USA) were vortexed vigorously for 1 min and gently stirred until phase separation (instead of allowed to stand). The protocol was adjusted to avoid cell sedimentation during phase separation, because ST44 is primarily encountered in long chains that tend to sediment (Nachtigall et al., 2019). After complete phase separation, the aqueous phase was carefully removed and the OD_{600} was measured.

The percentage of microbial adhesion to hexadecane (or % Hydrophobicity) was estimated as:

$$\%\ Hydrophobicity = \left(\frac{1 - A_1}{A_0}\right) \times 100 \quad (2)$$

Where A_0 is the initial absorbance of the cell suspension and A_1 is the absorbance after phase separation at 600 nm. Each sample was analyzed in triplicate.

2.5. Electrospray of probiotic solutions

Maltodextrin of Dextrose Equivalent 12 (Glucidex IT12, Roquette, Lestrem, France) was dispersed in demineralized water in a concentration of 85% w/v and stirred until homogeneously solubilized. Then ST44 probiotic cells (1.6×10^8 cells/mL) were introduced and stirred gently until they were fully dispersed.

The electrospray process was performed in horizontal mode. The maltodextrin–ST44 feed solution was loaded into a 10 mL syringe, connected to a metal needle and driven by a syringe pump (New Era Pump Systems, Inc., Farmingdale, NY, USA) at a flow rate of 0.03 mL/min. The electric field was established by a high voltage power supply (ES50P–10W, Gamma High Voltage Research, Inc., USA), which was connected to the electrospray needle and a stainless-steel collecting electrode (collector). The maltodextrin–ST44 capsules were collected on the collector (10 × 10 cm), which was placed at a distance of 10 cm from the end of the needle. One or two auxiliary ring-shaped electrodes (r = 4 cm) were placed between the needle and the collector at a distance of 2 cm, or 2 cm and 4 cm from the end of the needle, and each was connected to a high voltage power supply (ES50P–10W, Gamma High Voltage Research, Inc., USA). The auxiliary electrodes had a thickness of 0.5 mm and 1.25 mm respectively and were connected to the pole of the power supply with the same polarity as the electrospray needle (± 5 kV). When the electrospray needle was connected to the positive pole (+15 kV) of the DC high voltage power supply, the collector was connected to the negative pole (-5 kV), and the sample is referred to as "electrosprayed under positive polarity", and reversely for "electrosprayed under negative polarity". The absolute value of the electric potential is presented throughout this study, as |20 kV|.

The electrospray set-up was placed inside a polycarbonate chamber, where temperature (20 ± 1 °C) and relative humidity (RH = 20 ± 3%) were controlled by introducing nitrogen gas through a diffuser (Fig. 1).

2.6. Confocal laser scanning microscope

An Inverted Zeiss LSM-710 Confocal laser scanning microscope (Carl Zeiss MicroImaging GmbH, Jena, Germany) equipped with a diode laser (405 nm), argon laser (458, 488 and 514 nm), two HeNe lasers (543 and 633 nm), three detectors and one transmitted detector, was utilized.

The fluorescent dye Thiazole Orange, dye content~90% (Sigma-Aldrich, St. Louis, Missouri, USA) was dissolved in dimethyl sulfoxide (DMSO) at concentration 42 μmol/L and was used to stain the probiotic cells prior to encapsulation. The images were obtained at an excitation wavelength of 488 nm and emission bandpass filter between 505 and 550 nm. The samples were scanned at different focal planes employing the Z-series mode using the software ZEN 2009 (Carl Zeiss MicroImaging GmbH, Jena, Germany). The maximum intensity projections of the Z-stack series were reconstructed in a 2D image. Circles were drawn around the microcapsules to approximate the edge of the capsules and to facilitate imaging.

2.7. Differential scanning calorimetry

The glass transition temperature (Tg) of the electrosprayed microcapsules was determined by Modulated Differential Scanning Calorimetry (MDSC) experiments, following a previously described protocol (Dima et al., 2023). The DSC 250 (TA Instruments, New Castle, Delaware, USA), equipped with Refrigerated Cooling System 90, was utilized to obtain the thermograms of the samples. The heat flow and temperature calibration of the instrument was performed using distilled water (melting point (m.p.) = 0 °C; DHm = 334 J/g) and indium (m.p. = 156.5 °C; DHm = 28.5 J/g), and nitrogen gas at a flow rate of 50 mL/min

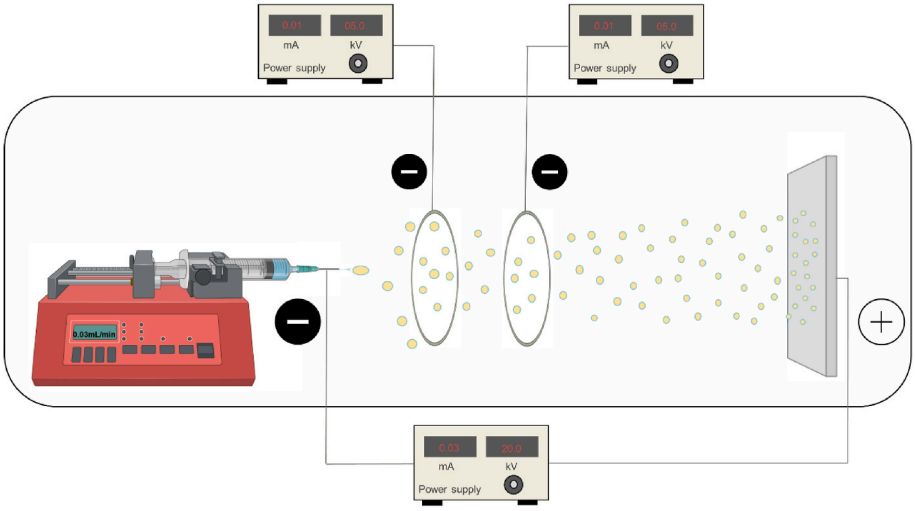

Fig. 1. Schematic representation of the negative polarity electrospray apparatus inside a polycarbonate chamber, consisting of a syringe pump, a syringe connected to a metal needle, two auxiliary ring-shaped electrodes, and a collecting electrode. High voltage power supplies were connected to the electrospray needle, auxiliary rings and collecting electrode.

was used as a carrier.

Electrosprayed microcapsules (immediately collected after processing), of approximately 5 mg, were placed in pre-weighted standard DSC aluminum pans (Tzero aluminum Hermetic pans, TA Instruments, USA) and were hermetically sealed. An empty hermetically sealed aluminum pan was used as reference. The microcapsules in the pans were initially equilibrated for 5 min at 10 °C, and then a heating ramp followed with 3 °C/min to 120 °C. The temperatures of the thermal scanning were set at least 30 °C below and above the expected Tg of the electrosprayed microcapsules, considering the Tg of maltodextrin DE12.

The Tg was determined from the midpoint temperature of the detected step change, operating the Trios software interfaced with the DSC 250 for the analysis. All measurements were done in triplicate and the Tg values were averaged.

2.8. Stability of microencapsulated ST44 probiotics during storage

The conditions for the stability of the microencapsulated ST44 were chosen based on a previously described protocol (Dima et al., 2023). Microcapsules containing ST44 electrosprayed with negative and positive polarities with and without 2 auxiliary ring-electrodes, and non-encapsulated *Streptococcus thermophilus* (reference sample), were stored in an incubating cabinet (Model KB 8400F, A/S Ninolab, Solrød Strand, Denmark) at a relative humidity of 35 ± 2% RH at 25 °C. The viability of the encapsulated and non-encapsulated ST44 probiotics as a function of time (0–14 days) was determined by Colony Forming Unit (CFU) analysis. More specifically, the electrosprayed microcapsules were dispersed in 0.85% w/v sodium chloride (NaCl) and 0.1% w/v peptone (tryptone) solution, homogenized by vortexing, and then 1 mL of appropriate decimal dilutions was pour-plated in M-17 agar (Merck KGaA, Darmstadt, Germany) plates supplemented with 10% w/v lactose. The M-17 agar plates were incubated at 37 °C under aerobic conditions for 2 days, and the cell viability was calculated as the average of 4 plates.

The Encapsulation Efficiency (*EE*) of the microcapsules was defined by determining the log of the number of viable cells inside the microcapsules (*N*) divided by the log of the number of viable cells in the initial solution (N_0):

$$EE\ (\%) = \frac{\log N}{\log N_0} \times 100 \tag{3}$$

2.9. Statistical analysis

Student's T-test was applied to determine the statistical significance among samples' Tg, using Excel software (Microsoft corporation). One-tailed unpaired *t*-test with 95% confidence interval was considered statistically significant ($p < 0.05$). The results are expressed as mean value ± Standard Deviation (SD).

2.10. Finite element modeling (FEM)

The numerical simulations were performed using a freeFEM++ simulator. The electric potential and electric field strength between the nozzle and collector electrode were analyzed by introducing one or two auxiliary ring electrodes. The calculations were carried out according to the described settings in section 2.3. The range of the mesh size was 6μm–1.9m for no ring, 5.4μm–1.87m for one ring, and 5.5μm–1.9m for two rings. In regard to boundary conditions, the electric potential was fixed to zero at the locations within 68.8 times the radius of the auxiliary ring electrode in the radial direction.

Assuming no or negligible current and a steady state, it was found from Maxwell's equations that the electric field *E* obeys:

$$\nabla \cdot \boldsymbol{E} = \frac{\rho}{\varepsilon_0} \tag{4}$$

$$\nabla \times \boldsymbol{E} = 0 \tag{5}$$

$$\boldsymbol{E} = -\nabla U \tag{6}$$

Where ρ is the charge density and ε_0 is the permittivity of vacuum. The field was found as the negative gradient of the electrostatic potential *U*. The condition $\nabla \times \nabla U = 0$ is automatically fulfilled.

Before starting electrospraying $\rho = 0$, so (4) and (5) can be expressed as:

$$-\Delta U = 0$$

More details about the freeFEM++ solution can be found in the Appendix A-Supplementary data.

3. Results and discussions

3.1. Morphology and surface properties of Streptococcus thermophilus (ST44)

The AFM images of the ST44 probiotic cells are presented in Fig. 2. Streptococci are spherical bacteria, which grow in chains due to the incomplete separation after division of the cells (Chhatwal and Graham, 2017). ST44 chaining phenotype can be noticed in Fig. 2 where the three types of septa emerging from septum synthesis can be clearly recognized. First, the nascent septum (a), which is situated halfway between the cell poles of the diplococcal dividing cells and originated from the constriction ring. Second, the intermediate septum (b), deriving from the progression of the septal peptidoglycan synthesis and additional compression of the cell walls. And third, the mature septum (c), which arises from the extension of the septum that connects the daughter cells together by a thin peptidoglycan filamentous, and is usually detected at the final stage of the division process (Layec et al., 2009).

According to the literature, ST44 is an aerotolerant anaerobe, Gram-positive, spherical, nonmotile coccus, which falls into to the thermophilic group of the lactic acid bacteria, presenting an optimum growth temperature of approximately 42 °C (Facklam, 2002). Based on Fig. 2, ST44 probiotic cells were ovoid-shaped with 1.095 ± 0.098 μm width and 0.747 ± 0.047 μm height (n = 5), similar to findings that have been reported in literature (Chhatwal and Graham, 2017; Guss and Delwiche, 1954).

As illustrated at Fig. 3, the cultivated ST44 presented a zeta potential

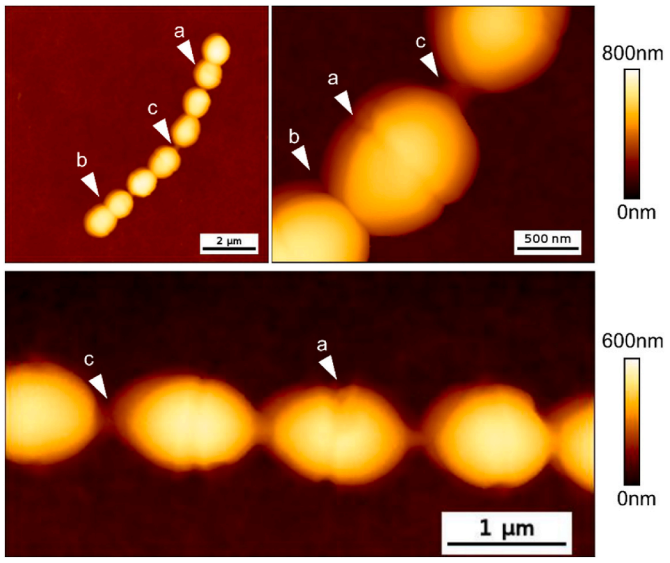

Fig. 2. ST44 chaining phenotype observed by Atomic Force Microscopy (AFM). The arrow heads indicate the nascent septum (**a**), the intermediate septum (**b**) and the mature septum (**c**).

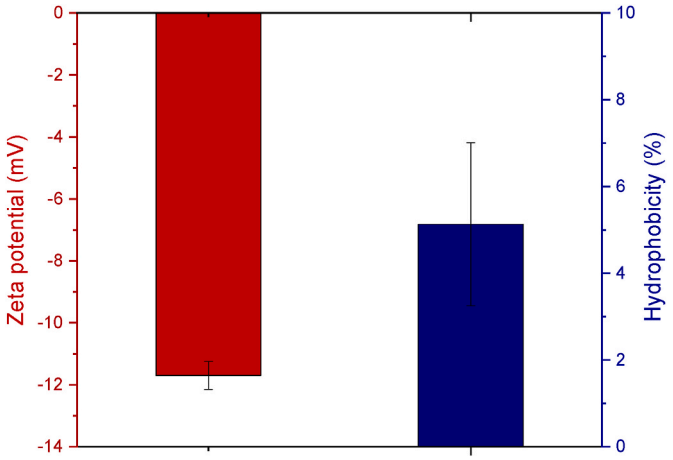

Fig. 3. Zeta potential and (%) Hydrophobicity of ST44 in KH_2PO_4 at pH = 6.

of −11.7 ± 0.45 mV. The electronegative character of ST44 at neutral pH is due to cell surface molecules, including wall teichoic acids (WTA) and lipo-teichoic acids (LTA), whose phosphodiester bonds confer a negative charge to the whole polymers and subsequently to the probiotics (Dahmane et al., 2018).

The cell surface hydrophobicity of the cultivated ST44 was also evaluated, by studying the adhesion of the probiotics to hexadecane (Fig. 3). At pH = 6, ST44 showed an affinity to hexadecane of 5.1 ± 1.9%, suggesting a hydrophilic cell surface character. The hydrophilic character of ST44 (4.4% after cultivation) have been previously reported and correlated with the formation of (capsular) exopolysaccharides (EPS) (Nachtigall et al., 2019). It should be noted that the long chains of ST44 tend to sediment due to their high mass and could lead to discrepancies in the hydrophobicity measurements. Thus, the protocol was adjusted according to Nachtigall et al., to avoid cell sedimentation during phase separation and to estimate the surface hydrophobicity more accurately (Nachtigall et al., 2019).

3.2. *Effect of electric field charge polarity and auxiliary electrodes on the ST44 "organization" within the microcapsules*

The distribution of coccus-shaped ST44 probiotics within the electrosprayed maltodextrin microcapsules, when either negative or positive polarity was applied on the electrospray needle, was monitored by confocal laser scanning microscopy (CLSM) (Fig. 4). To assist the visualization of the distribution of the encapsulated ST44, the electrosprayed microcapsules with higher diameter are presented. The microcapsules produced without the auxiliary electrode showed a diameter between 10 and 60 μm for positive and 40–100 μm for negative polarity. When 1 auxiliary ring electrode was used, the corresponding sizes were 20–50 μm and 40–80 μm.

The "organization" of the probiotic cells towards the core of the microcapsules, was noted when negative polarity was employed at the electrospraying needle. Conversely, the probiotics were allocated towards the surface of the electrosprayed microcapsules when a positive polarity was applied at the needle (Fig. 4). The encapsulation and distribution of negatively charged ST44 towards the core or the shell of the microcapsules is due to Coulombic forces within the DC electric field. Either electrostatic repulsion or attraction between the negatively surface charged ST44 cells at pH = 6 and the negatively or positively charged electric field at the needle walls respectively, direct the "organization" of the charged ST44 cells within the electrosprayed microcapsules.

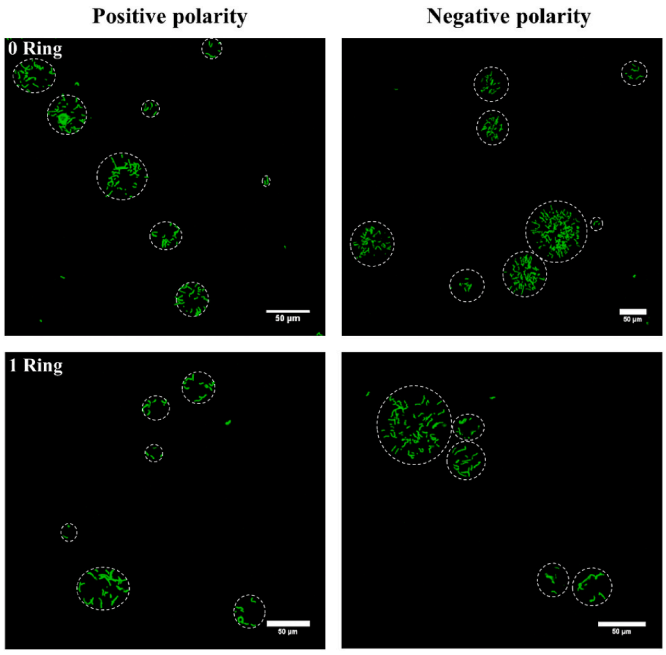

Fig. 4. Confocal laser scanning microscopy (CLSM) micrographs showing the distribution of ST44 cells within microcapsules electrosprayed at |20 kV| with different polarities. The edge of the microcapsules is represented by white circles.

3.3. *Glass transition temperature of electrosprayed microcapsules*

The effect of the polarity of the electric field (at |20kV|), as well as the addition of auxiliary ring-electrodes, on the glass transition temperature (Tg) of the maltodextrin–ST44 electrosprayed microcapsules is depicted in Fig. 5.

The Tg of the maltodextrin–ST44 electrosprayed microcapsules with negative polarity were characterized by statistically significantly higher Tg values than the microcapsules electrosprayed with a positive polarity, in accordance with the previous study (Dima et al., 2023). More specifically, the microcapsules produced using I20kVI with one auxiliary ring electrode and negative polarity, presented an approximately 12 °C higher Tg, compared to the corresponding electrosprayed microcapsules

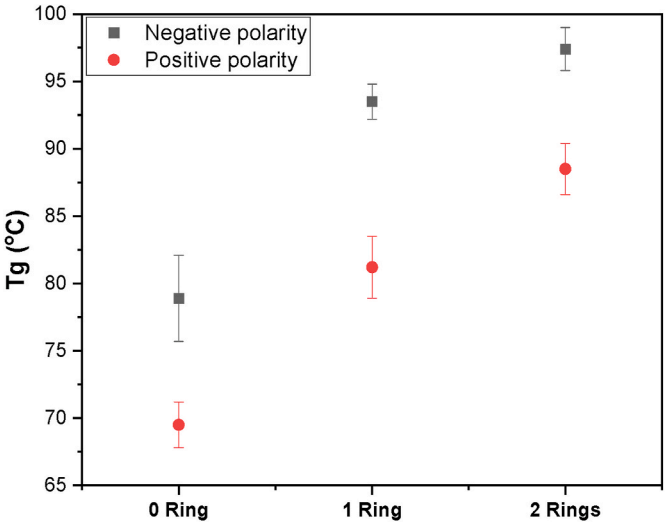

Fig. 5. Effect of electrospray polarity, and auxiliary ring-electrodes on the glass transition temperature (Tg) of electrosprayed maltodextrin microcapsules encapsulating ST44.

with positive polarity. When two complementary ring-electrodes were utilized between the electrospraying nozzle and the collector, the Tg of the negative polarity electrosprayed microcapsules approached 100 °C and was approximately 9 °C higher than the respective positive polarity electrosprayed microcapsules. The higher Tg values using negative polarity electric field arise from the "organization" of the negatively surface charged ST44 probiotic cells towards the core of the initially formed droplets. The subsequent accumulation of the solvent near to the highly charged microcapsules' surface, leads to enhanced evaporation of the solvent during electrospray. This enhanced water evaporation with subsequent decrease of the moisture content, leads to higher Tg values for the microcapsules electrosprayed using negative polarity, compared to the microcapsules electrosprayed using positive polarity.

The microcapsules produced using the two auxiliary ring-electrode electrospray setup, presented statistically higher glass transition temperature values compared to the microcapsules electrosprayed with one or no auxiliary electrode. More specifically, the microcapsules produced at negative polarity with two ring-electrodes presented a 4 °C higher Tg than the microcapsules produced with one ring-electrode, and 19 °C higher Tg compared to the microcapsules produced with no auxiliary electrode. When positive polarity and two auxiliary ring-electrode setup was utilized, the corresponding Tg differences were 7 °C (with one ring-electrode) and 19 °C higher (with no ring-electrode).

Consequently, both the applied electric field charge polarity on the nozzle and the utilization of auxiliary ring-electrodes significantly affected the glass transition temperature of the electrosprayed microcapsules, due to the presence of the surface charged probiotics and the enhancement of the electric field by the ring-electrodes.

3.4. Numerical simulation of electric field (FEM)

3.4.1. Effect of auxiliary ring electrodes on the electric field strength and potential distribution

The computational Finite Element Method (FEM) was employed for the numerical simulation of the electric field strength and electric potential distribution for the electrospray process. A qualitative examination of the deformation of the electric field between the electrospray needle and the collector, with and without the auxiliary ring-electrodes is presented in Fig. 6. It can be noticed that the addition of the ring-shaped electrodes increased the strength of the electric field in the vicinity of the collector and decreased in the proximity of the nozzle.

It has been previously reported that the utilization of an additional ring electrode decreased the magnitude of the electric field around the tip of the nozzle (Neubert et al., 2012). Furthermore, it was demonstrated by previous FEM simulations, that the addition of a ternary ring-shaped electrode altered the electric field lines, increasing the strength of the electric field in the direction of the central axis. More specifically, the spatial electric potential was increased closer to the counter electrode, being in agreement with the current findings in Fig. 6 (Kuwahata et al., 2020).

A quantitative evaluation of the electric field strength and the potential along the center line from the needle to the center of the collector was also estimated through FEM. It can be noticed that a substantially stronger electric field of up to 142 kV/m at the collector was calculated when two auxiliary rings were introduced in the electrospray setup. However, lower values were found when one auxiliary ring and no ring-electrode was utilized, noting an electric field strength of approximately 104 kV/m and 69 kV/m, respectively (Fig. 7A).

In addition, differences regarding the potential can also be clearly noticed between the samples with no, one and two ring-electrodes (Fig. 7B). The results from FEM indicate that the electric potential distribution around the nozzle electrode approached the potential of the nozzle with the addition of the ring-shaped electrodes. Similar findings have been previously reported, where the electric potential distribution around the nozzle increased (Kuwahata et al., 2020).

Thus, the numerical simulation of the electric field gradients between the needle and the collector revealed that a locally stronger electric field (close to collector) is formed when auxiliary ring electrodes were utilized. This is in agreement with the higher glass transition temperatures and enhanced solvent evaporation observed using the complementary ring-electrodes.

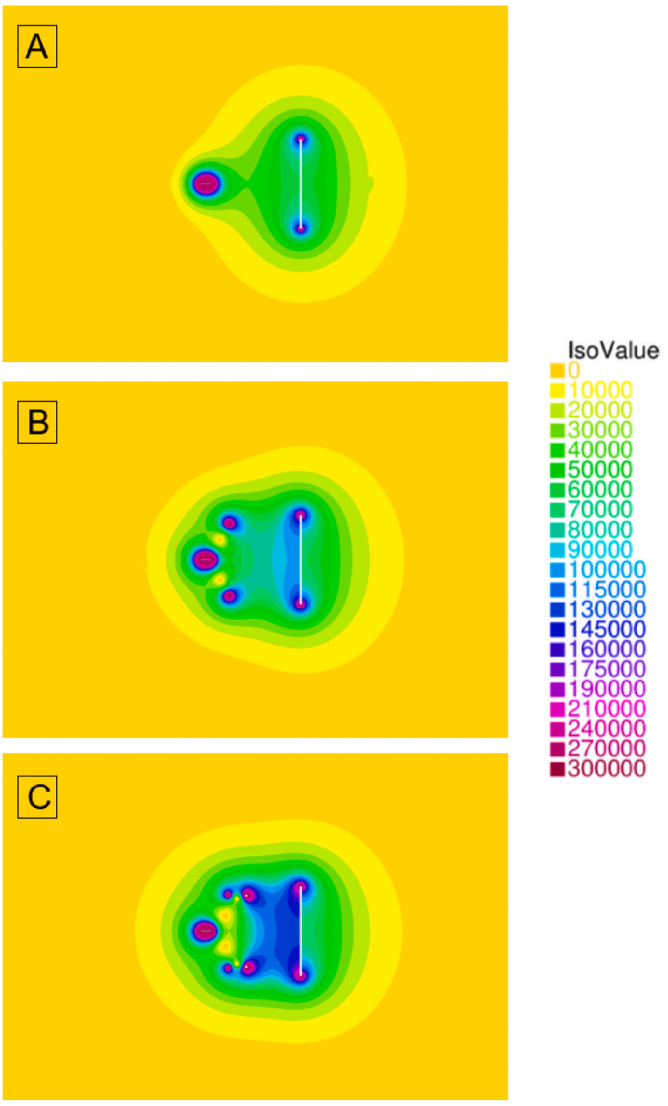

Fig. 6. Axisymmetric FEM analysis of the electric field strength for electrospray processing (|20 kV|) using negative polarity at the needle (A) Without the auxiliary ring-electrode, (B) With 1 ring-electrode, and (C) With 2 ring-electrodes. The colors represent the electric field strength in V/m (Iso value).

3.4.2. Effect of auxiliary ring electrodes on the controlled deposition of capsules

A qualitative assessment of the deformation of the electric field lines between the electrospray needle and the collector, with and without the auxiliary ring-electrodes is also presented in Fig. 8. The FEM simulation revealed that the electric field streamlines between the tip of the nozzle and the collector, were narrowed down when auxiliary ring-electrodes were utilized, designating that the deposition area of the capsules can be focused.

This result could be justified due to the more homogeneous electric field distribution when auxiliary ring-electrodes are used. Kuwahata et al., also reported that the ring electrode facilitated the focusing of the spray plume and the controlling of the electrospray film deposition of PLGA (Kuwahata et al., 2020). Moreover, Neubert et al., simulated and

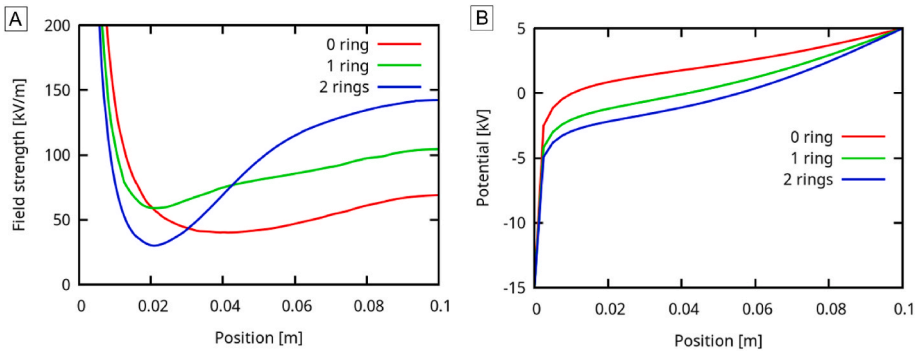

Fig. 7. Electric field strength (A) and Potential (B) at the center line between the needle and the center of the collector when negative polarity was used.

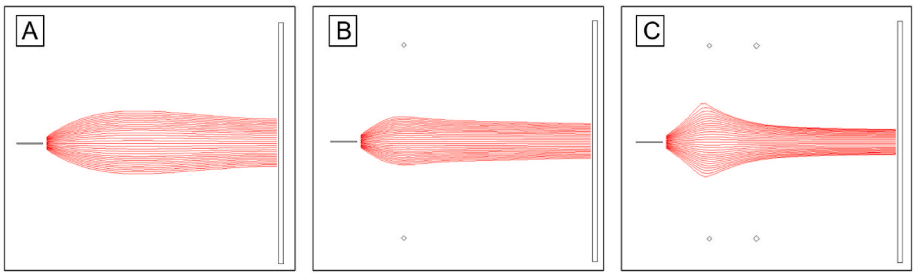

Fig. 8. Axisymmetric FEM analysis of the electric field lines for electrospray processing (|20 kV|) using negative polarity at the needle (A) Without the auxiliary ring-electrode, (B) With 1 ring-electrode, and (C) With 2 ring-electrodes.

experimentally confirmed, that the addition of a ring electrode focused the collection of Nylon-6, PLACL, and PVC electrospun fibers on the substate (Neubert et al., 2012).

3.5. Stability and cell viability of microencapsulated probiotic cells

The log loss of ST44 viability over time is displayed in Fig. 9. A significantly higher viability (~1.5 times) after 7 days of storage at 25 °C and 35% RH, was noticed for the probiotics encapsulated using negative polarity compared to the corresponding probiotics encapsulated using positive polarity, either when no ring or when 2 ring-electrodes were utilized. The capsules electrosprayed in a 2-ring-electrode setup with negative polarity presented 5 times higher ST44 viability compared to the cells electrosprayed with positive polarity, after 14 days of storage. Moreover, it was observed that the higher Tg of the capsules electrosprayed with 2 ring-electrodes (either positive or negative polarity) further enhanced the ST44 stability, probably due to the lower moisture content, as seen previously, denoting approximately 2 times higher ST44 viability after 3 and 7 days of storage. Additionally, the ST44 encapsulated with negative polarity (no ring-electrodes) presented 85.7, 82.3, and 34.3 times higher viability compared to the non-encapsulated after 3, 7 and 14 days of storage, respectively. Furthermore, it should be mentioned that the encapsulation efficiency of the microcapsules was similar for both polarities (65.0 ± 1.6% and 68.5 ± 4.6% for positive and negative polarities, respectively).

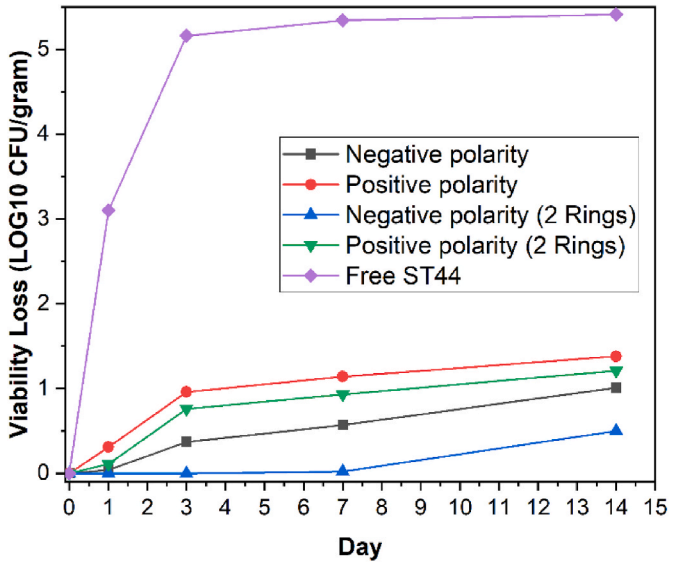

Fig. 9. Log loss of viability over time (25 °C and 35 ± 2 %RH) of encapsulated ST44 probiotic cells within electrosprayed maltodextrin microcapsules using different electric field polarities and 2 auxiliary ring-electrodes, and of non-encapsulated (free) ST44 cells.

Hence, a higher viability up to about 14 days of storage was displayed for ST44 encapsulated utilizing negative polarity, compared to the cells electrosprayed using positive polarity, while even more pronounced viability enhancement was observed for the capsules electrosprayed with the auxiliary ring-electrodes. The latter ascends from the "organization" of the cells within the core of the electrosprayed microcapsules using negative polarity, as well as the decreased moisture content of these microcapsules, which offer superior conditions for the stability of the encapsulated cells (Dima et al., 2023). Consequently, regardless of the shape, the size and the surface hydrophobicity of the encapsulated probiotic cells by electrospray processing, their stability can be effectively controlled by modulating the polarity of the external electric field.

4. Conclusions

It the current study the encapsulation of the coccus-shaped and hydrophilic *Streptococcus thermophilus* (ST44) within electrosprayed maltodextrin microcapsules, was enhanced using negatively charged electrospray needle, where ST44 cells were "organized" within the microcapsules depending on the electric field charge polarity. It was

concluded that the surface charge of the probiotic cells (rather than their size, shape, and surface properties) was responsible for their "organization" within the electrosprayed microcapsules. The generated electrostatic forces between the surface-charged probiotic cells and the applied polarity on the electrospray nozzle allowed not only to control the "organization" of the cells within the microcapsules, but also to influence the solvent evaporation, and to enhance their viability and stability.

The computational Finite Element Method (FEM) was also employed to evaluate the electric field strength, which was found that substantially increased when auxiliary ring-shaped electrodes were employed, contributing to further increase of the glass transition temperature values. Correlations among the focused deposition of the electrosprayed microcapsules and the deformation of the electric field streamlines for the different auxiliary electrodes, were also assessed through numerical simulation.

Overall, this study presents a novel method to increase electrospraying controllability, by manipulating the encapsulation of surface charged probiotic cells within electrosprayed microcapsules, and by controlling the deposition of the microcapsules on the collector, utilizing the appropriate polarity of the electric field and auxiliary ring-electrodes.

CRediT authorship contribution statement

Panagiota Dima: Conceptualization, Methodology, Validation, Investigation, Writing – original draft. **Peter Reimer Stubbe:** Methodology. **Ana C. Mendes:** Conceptualization, Formal analysis, Visualization, Investigation, Writing – review & editing, Supervision. **Ioannis S. Chronakis:** Conceptualization, Formal analysis, Visualization, Resources, Writing – review & editing, Supervision.

Declaration of competing interest

The authors declare the following financial interests/personal relationships which may be considered as potential competing interests:

Ioannis S. Chronakis reports that the financial support was provided by the Innovation Fund Denmark. Panagiota Dima, Peter Reimer Stubbe, Ana C. Mendes, Ioannis S. Chronakis have a patent application; "Method of Encapsulation by Electrohydrodynamics" (Filed patent No. EP22179401.9) pending to Chr. Hansen.

Data availability

The data that has been used is confidential.

Acknowledgments

The authors gratefully acknowledge the support provided by the Innovation Fund Denmark (PROBIO project - 7076-00053B). Furthermore, the authors wish to thank Dr. Alexander Dulebo for assistance with AFM measurements (Bruker Nano GmbH), and Chr. Hansen A/S for valuable discussions.

Appendix A. Supplementary data

Supplementary data to this article can be found online at https://doi.org/10.1016/j.crfs.2023.100620.

References

Chhatwal, G.S., Graham, R., 2017. Streptococcal diseases. In: International Encyclopedia of Public Health. Elsevier, pp. 87–97. https://doi.org/10.1016/B978-0-12-803678-5.00434-3.

Dahmane, N., Robert, E., Deschamps, J., Meylheuc, T., Delorme, C., Briandet, R., Leblond-Bourget, N., Guédon, E., Payot, S., 2018. Impact of cell surface molecules on conjugative transfer of the integrative and conjugative element ICE St3 of *Streptococcus thermophilus*. Appl. Environ. Microbiol. 84, 1–16. https://doi.org/10.1128/AEM.02109-17.

Deepika, G., Green, R.J., Frazier, R.A., Charalampopoulos, D., 2009. Effect of growth time on the surface and adhesion properties of *Lactobacillus rhamnosus* GG. J. Appl. Microbiol. 107, 1230–1240. https://doi.org/10.1111/j.1365-2672.2009.04306.x.

Dertli, E., Mayer, M.J., Narbad, A., 2015. Impact of the exopolysaccharide layer on biofilms, adhesion and resistance to stress in *Lactobacillus johnsonii* FI9785. BMC Microbiol. 15, 1–9. https://doi.org/10.1186/s12866-015-0347-2.

Dima, P., Gulbinas, G., Stubbe, P.R., Mendes, A.C., Chronakis, I.S., 2022. Electrohydrodynamic drying of probiotics. Innov. Food Sci. Emerg. Technol. 82, 103201 https://doi.org/10.1016/j.ifset.2022.103201.

Dima, P., Stubbe, P.R., Mendes, A.C., Chronakis, I.S., 2023. Electric field charge polarity triggers the organization and promotes the stability of electrosprayed probiotic cells. Food Hydrocolloids 139, 108549. https://doi.org/10.1016/j.foodhyd.2023.108549.

Facklam, R., 2002. What happened to the streptococci: overview of taxonomic and nomenclature changes. Clin. Microbiol. Rev. 15, 613–630. https://doi.org/10.1128/CMR.15.4.613-630.2002.

Gan, Y., Jiang, Z., Li, H., Luo, Y., Chen, X., Shi, Y., Yan, Yuying, Yan, Yunfei, 2019. A comparative study on droplet characteristics and specific charge of ethanol in two small-scale electrospray systems. Sci. Rep. 9, 1–12. https://doi.org/10.1038/s41598-019-55223-6.

Gan, Y., Zhang, X., Li, H., Tong, Y., Zhang, Y., Shi, Y., Yang, Z., 2016. Effect of a ring electrode on the cone-jet characteristics of ethanol in small-scale electro-spraying combustors. J. Aerosol Sci. 98, 15–29. https://doi.org/10.1016/j.jaerosci.2016.05.001.

Guss, M.L., Delwiche, E.A., 1954. *Streptococcus thermophilus*. J. Bacteriol. 67, 714–717. https://doi.org/10.1128/jb.67.6.714-717.1954.

Jaworek, A., Sobczyk, A.T., Krupa, A., 2018. Electrospray application to powder production and surface coating. J. Aerosol Sci. 125, 57–92. https://doi.org/10.1016/j.jaerosci.2018.04.006.

Kuwahata, Y., Takehara, H., Ichiki, T., 2020. Comprehensive study on electrospray deposition in the single Taylor cone-jet mode by changing the spatial electric potential using a ring-shaped ternary electrode. AIP Adv. 10 https://doi.org/10.1063/1.5142317.

Layec, S., Gérard, J., Legué, V., Chapot-Chartier, M.-P., Courtin, P., Borges, F., Decaris, B., Leblond-Bourget, N., 2009. The CHAP domain of Cse functions as an endopeptidase that acts at mature septa to promote *Streptococcus thermophilus* cell separation. Mol. Microbiol. 71, 1205–1217. https://doi.org/10.1111/j.1365-2958.2009.06595.x.

Martinović, A., Cocuzzi, R., Arioli, S., Mora, D., 2020. *Streptococcus thermophilus*: to survive, or not to survive the gastrointestinal tract, that is the question. Nutrients 12, 2175. https://doi.org/10.3390/nu12082175.

Mendes, A.C., Chronakis, I.S., 2021. Electrohydrodynamic encapsulation of probiotics: a review. Food Hydrocolloids 117, 106688. https://doi.org/10.1016/j.foodhyd.2021.106688.

Nachtigall, C., Weber, C., Rothenburger, S., Jaros, D., Rohm, H., 2019. Test parameters and cell chain length of *Streptococcus thermophilus* affect the microbial adhesion to hydrocarbons assay: a methodical approach. FEMS Microbiol. Lett. 366, 1–7. https://doi.org/10.1093/femsle/fnz150.

Neubert, S., Pliszka, D., Góra, A., Jaworek, A., Wintermantel, E., Ramakrishna, S., 2012. Focused deposition of electrospun polymer fibers. J. Appl. Polym. Sci. 125, 820–827. https://doi.org/10.1002/app.35578.

Niamah, A.K., Gddoa Al-Sahlany, S.T., Ibrahim, S.A., Verma, D.K., Thakur, M., Singh, S., Patel, A.R., Aguilar, C.N., Utama, G.L., 2021. Electro-hydrodynamic processing for encapsulation of probiotics: a review on recent trends, technological development, challenges and future prospect. Food Biosci. 44, 101458 https://doi.org/10.1016/j.fbio.2021.101458.

Ozturk, B., Elvan, M., Ozer, M., Tellioglu Harsa, S., 2021. Effect of different microencapsulating materials on the viability of *S. thermophilus* CCM4757 incorporated into dark and milk chocolates. Food Biosci. 44, 101413 https://doi.org/10.1016/j.fbio.2021.101413.

Padmanabhan, A., Tong, Y., Wu, Q., Lo, C., Shah, N.P., 2020. Proteomic analysis reveals potential factors associated with enhanced EPS production in *Streptococcus thermophilus* ASCC 1275. Sci. Rep. 10, 807. https://doi.org/10.1038/s41598-020-57665-9.

Pakroo, S., Ghion, G., Tarrah, A., Giacomini, A., Corich, V., 2021. Effects of 2′-fucosyllactose-based encapsulation on probiotic properties in *Streptococcus thermophilus*. Appl. Sci. 11, 5761. https://doi.org/10.3390/app11135761.

Parvez, S., Malik, K.A., Ah Kang, S., Kim, H.-Y., 2006. Probiotics and their fermented food products are beneficial for health. J. Appl. Microbiol. 100, 1171–1185. https://doi.org/10.1111/j.1365-2672.2006.02963.x.

Si, T., Zhang, L., Li, G., Roberts, C.J., Yin, X., Xu, R., 2013. Experimental design and instability analysis of coaxial electrospray process for microencapsulation of drugs and imaging agents. J. Biomed. Opt. 18, 075003 https://doi.org/10.1117/1.jbo.18.7.075003.

Terpou, A., Papadaki, A., Lappa, I., Kachrimanidou, V., Bosnea, L., Kopsahelis, N., 2019. Probiotics in food systems: significance and emerging strategies towards improved viability and delivery of enhanced beneficial value. Nutrients 11, 1591. https://doi.org/10.3390/nu11071591.

Verdoold, S., Agostinho, L.L.F., Yurteri, C.U., Marijnissen, J.C.M., 2014. A generic electrospray classification. J. Aerosol Sci. 67, 87–103. https://doi.org/10.1016/j.jaerosci.2013.09.008.

Vodnar, D.C., Socaciu, C., Rotar, A.M., Stănilă, A., 2010. Morphology, FTIR fingerprint and survivability of encapsulated lactic bacteria (*Streptococcus thermophilus* and *Lactobacillus delbrueckii* subsp. *bulgaricus*) in simulated gastric juice and intestinal

juice. Int. J. Food Sci. Technol. 45, 2345–2351. https://doi.org/10.1111/j.1365-2621.2010.02406.x.
Xie, J., Wang, C.H., 2007. Electrospray in the dripping mode for cell microencapsulation. J. Colloid Interface Sci. 312, 247–255. https://doi.org/10.1016/j.jcis.2007.04.023.
Zhang, J., Liu, M., Xu, J., Qi, Y., Zhao, N., Fan, M., 2020. First insight into the probiotic properties of ten *Streptococcus thermophilus* strains based on in vitro conditions. Curr. Microbiol. 77, 343–352. https://doi.org/10.1007/s00284-019-01840-3.
Zhao, S., Castle, G.S.P., Adamiak, K., 2005. Comparison of conduction and induction charging in liquid spraying. J. Electrostat. 63, 871–876. https://doi.org/10.1016/j.elstat.2005.03.048.